Aerosol Science and Technology, 38(S1):253–264, 2004

ISSN: 0278-6826 print / 1521-7388 online
DOI: 10.1080/02786820390229570

Characterizing Physical Processes

Nucleation Events During the Pittsburgh Air Quality Study: Description and Relation to Key Meteorological, Gas Phase, and Aerosol Parameters

Charles O. Stanier, Andrey Y. Khlystov, and Spyros N. Pandis
Department of Chemical Engineering, Carnegie Mellon University, Pittsburgh, Pennsylvania

During the Pittsburgh Air Quality Study (PAQS) aerosol size distributions between 3 nm and 680 nm were measured between July 2001 and June 2002. These distributions have been analyzed to assess the importance of nucleation as a source of ultrafine particles in Pittsburgh and the surrounding areas. The analysis shows nucleation on 50% of the study days and regional-scale formation of ultrafine particles on 30% of the days. Nucleation occurred during all seasons, but it was most frequent in fall and spring and least frequent in winter. Regional nucleation was most common on sunny days with below average $PM_{2.5}$ concentrations. Local nucleation events were usually associated with elevated SO_2 concentrations. The observed nucleation events ranged from weak events with only a slight increase in the particle number to relatively intense events with increases of total particle counts between 50,000 cm^{-3} up to 150,000 cm^{-3}. Averaging all days of the study, days with nucleation events had number concentrations peaking at around noon at about 45,000 cm^{-3}. This is compared to work days without nucleation, when the daily maximum was 8 am at 23,000 cm^{-3}, and to weekends without nucleation, when the daily maximum was at noon at 16,000 cm^{-3}. Twenty-four-hour average number concentrations were approximately 40% higher on days with nucleation compared to those without. Nucleation was typically observed starting around 9 am EST, although the start of nucleation events was later in winter and earlier in summer. The nucleation events are fairly well correlated with the product of [UV intensity $*$ SO_2 concentration] and also depend on the effective area available for condensation. This indicates that H_2SO_4 is a component of the new particles. Published correlations for nucleation by binary H_2SO_4—H_2O cannot explain the observed nucleation frequency and intensity, suggesting that an additional component (perhaps ammonia) is participating in the particle formation.

Received 23 October 2002; accepted 5 March 2003.

This research was conducted as part of the Pittsburgh Air Quality Study, which was supported by the US Environmental Protection Agency under contract R82806101 and the US Department of Energy National Energy Technology Laboratory under contract DE-FC26-01NT41017. The authors also wish to thank Hiromu Sakurai, Peter McMurry, and the Minnesota Particle Technology Laboratory for their help with the ultrafine CPC testing.

Address correspondence to Spyros Pandis, Department of Chemical Engineering, Carnegie Mellon University, 5000 Forbes Ave., Pittsburgh, PA 15213, USA. E-mail: spyros@andrew.cmu.edu

INTRODUCTION

The creation of new particles by homogenous nucleation of gas-phase atmospheric components is an important atmospheric process. Together with primary particle emission, nucleation is responsible for maintaining the number concentration of particles throughout the atmosphere. Nucleation affects climate and visibility by changing the size distribution of airborne particles (Charlson et al. 1987; Kulmala et al. 2000). The formation of ultrafine particles and the condensation of secondary aerosol components on them may impact human health, as ultrafine particles are likely to cause adverse health effects disproportionate to their mass (Oberdoster et al. 1995; Schwartz et al. 1996; Peters et al. 1997).

Until recently, nucleation was assumed to be limited to clean areas of the atmosphere such as the free troposphere. However, a number of recent studies at both rural and urban sites around the world have reported frequent nucleation events (Allen et al. 1999; Harrison et al. 1999a, b; Harrison et al. 2001; Shi et al. 2001; Woo et al. 2001). Woo et al. (2001) found elevated levels of 3–10 nm particles in Atlanta, with highest frequencies in spring and summer. Birmili et al. (2001) measured elevated ultrafine concentrations in continental Germany in April as well. In both the German and Atlanta studies, nucleation occurred around midday with concentrations of NO_x elevated prior to many of the nucleation events and SO_2 elevated during the events (Woo et al. 2001).

Atmospheric homogeneous nucleation has been the subject of many theoretical and experimental studies. It is recognized

that there are two important steps to the production of new particles that can grow to detectable size (Zhang and Wexler 2002; Kerminen 1999). The first step is the formation of an initial nucleus, and the second step is the growth of the particles to larger sizes. A number of mechanisms have been proposed as candidates for the initial nucleus formation step based on observations and theoretical considerations, including (1) homogeneous binary nucleation of sulfuric acid and water (Weber et al. 1999); (2) homogeneous ternary nucleation of ammonia-water-sulfuric acid (Eisele and McMurry 1997; Kulmala et al. 2001; O'Dowd et al. 1999); (c) homogenous nucleation of low vapor pressure organic compounds (O'Dowd et al. 2002); (d) ion-induced nucleation (Kim et al. 2002). The second step in forming detectable new particles, growth, is also uncertain. These particles can grow by condensation of sulfuric acid or by self-coagulation. Both of these processes are relatively inefficient, and additional growth mechanisms have been proposed (Kerminen 1999). The limited experimental evidence indicates a potential role for organic compounds (Novakov and Penner 1993; Rivera-Carpio et al. 1996). Recent work considers the potential for heterogenous reactions of SO_2 (Kerminen 1999) and organic compounds (Kerminen 1999; Jang and Kamens 2001; Zhang and Wexler 2002) to significantly contribute to growth.

Steps toward a better understanding of tropospheric nucleation include: (a) elucidation of the mechanism responsible for the initial nuclei formation in different environments; (b) identification of the chemical compounds responsible for growth; (c) determination of the geographic scope, frequency, strength, and impact of tropospheric nucleation.

The goal of this work is to describe the nucleation events observed during the Pittsburgh Air Quality Study (PAQS) from July 2001 to June 2002. Analysis of the particle size distributions during this period shows over 100 days with nucleation activity. The gas, aerosol phase concentrations, and meteorological conditions associated with nucleation in Pittsburgh are also discussed.

Identification of initial nuclei and condensing species chemistry is ongoing and will be discussed in a subsequent article.

EXPERIMENTAL

All measurements were conducted as part of the PAQS, a multidisciplinary air pollution study designed to characterize fine particulate matter around Pittsburgh, evaluate next-generation aerosol monitoring instrumentation, elucidate source-receptor relationships, and improve understanding of atmospheric processes governing aerosol concentrations.

The bulk of the gas and particle measurements discussed in this article were conducted at the main PAQS sampling location in a park 5 km east (downwind) of downtown Pittsburgh (Figure 1). Two SMPS systems (TSI 3936L10 and TSI 3936N25) were operated at this location continuously. These instruments measured the size distribution of particles from 3 nm to 680 nm. The SMPS systems were a part of the dry-ambient aerosol sizing system (DAASS) (Stanier et al. 2002) and were specially configured to alternate between ambient RH samples and dried samples. The differential mobility analyzers (DMAs) and most of the inlet tubing were kept at near ambient temperature to avoid volatilization of aerosols. Portions of the inlet were maintained at above 9°C at all times because they shared an enclosure with the condensation particle counters (CPCs). This sampling location was 0.5 km from the nearest major city street and 1.1 km from the nearest highway. A small coal-fired heating plant operated 0.8 km from the site. Its plume impacted the sampling site occasionally but did not typically contain nuclei mode particles.

Another SMPS system (TSI 3071/3010) was located 38 km upwind from the main site in Florence, Pennsylvania during part of winter and spring 2002. The SMPS was sampling dried aerosol size distributions in the size range 12–280 nm. The data from the rural site were used to asses the regional homogeneity of the events.

Other instruments deployed as part of the PAQS and used to understand nucleation in this work include: O_3, SO_2, NO_2/NO, and CO monitors, a tapered element oscillating microbalance (TEOM), solar radiation, and met station. For PAQS, 10 min averaged $PM_{2.5}$ data were used from the TEOM. The TEOM operated at 30°C to minimize volatilization of nitrate and organic compounds, and the sample equilibration system was used to dry the aerosol stream prior to the mass measurement. The complete list of instrumentation used to generate the data set for nucleation events is listed in Table 1.

RESULTS AND DISCUSSION

Around 50% of the study days (July 2001 to June 2002) were characterized by nucleation events. Of these, about 60% showed a characteristic growth pattern from the nuclei mode to 30–100 nm over the course of several hours. During the other 40% of the nucleation events the sub-10 nm particles did not appear to grow to larger sizes. The events varied in intensity from weak increases in the ultrafine and nuclei mode particle counts to intense events which increased the overall number concentration from 10,000–20,000 per cm^3 to over 100,000 per cm^3 in a few hours. As an example of the contrast between days with and without nucleation, Figure 2 depicts the size distributions measured during 10 August and 11 August 2001. Figures 2a and b show evolution of the size distributions, while Figure 2c indicates the integrated particle concentration. On 10 August there was no detectable nucleation activity, while an intense nucleation event was observed around 9 AM EST on 11 August, followed by rapid growth of the particles to a size around 100 nm. Missing size distributions in Figure 2 correspond to maintenance of the particle-sizing instruments in some cases, and data flagged as invalid in other cases. Data was typically flagged invalid due to occasional communication errors between the data acquisition system and the particle-sizing instruments.

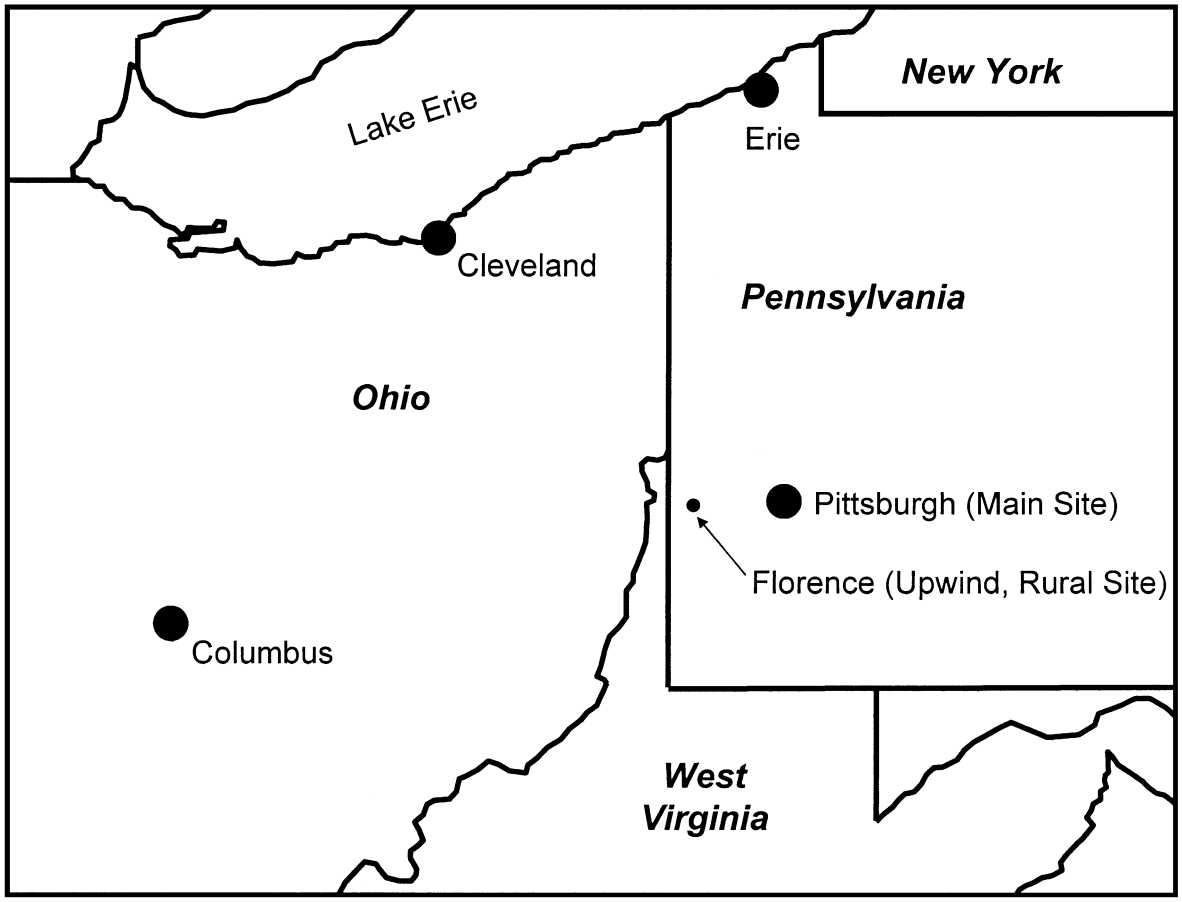

Figure 1. Map of Pittsburgh (main urban site) and Florence (rural upwind site).

Classification of Events

The size distributions from the study were first analyzed to determine the frequency of nucleation events. The analysis was done by examining the evolution of size distributions on each day of the study and various time series, including those of total number concentration, nuclei mode number concentration, aerosol mass (TEOM), meteorological parameters, and gas phase concentrations of CO, NO, NO_2, O_3, and SO_2.

The most important marker for nucleation was a significant increase in the nuclei mode particle count, defined as particles from the lower detection limit of 3 nm up to 10 nm, referred to as N_{10} in this work. Once a significant increase in N_{10} was seen in the particle count time series, additional characteristics of the data were examined to rule out primary particle sources, such as vehicular traffic, which also produce particles smaller than 10 nm. Traffic was fairly easy to screen out, as it usually has a weaker signal than most nucleation events. Diurnally averaged number concentrations during nucleation days and nonnucleation weekdays and weekends are shown in Figure 3. The mode of the traffic-related size distribution was consistently 15–20 nm, with most of the contribution to N_{10} between 6 and 10 nm. The traffic influence usually increased N_{10} from a background level of around 2,000 cm^{-3} to an early morning level of 7,500 cm^{-3} (Figure 3a). Finally, traffic was usually correlated with NO and CO and independent of solar radiation.

Once vehicular traffic was ruled out as the cause of a particular increase in N_{10}, the event was classified as a "short-lived" event, or a "regional" event following the approach by Shi (2003). Regional events were characterized by an increase in N_{10} followed by the growth of the nuclei mode to larger sizes, such as that shown in Figure 2 for 11 August. These growth events, lasting several hours, are called regional because throughout the day different air parcels are arriving at the site. If nucleation happened at a given time but was confined to a small area close by the site, the growing mode would disappear once air parcels began arriving at the site from outside the nucleation zone. The other group, classified as "short-lived" events, were characterized by an increase and then a decrease in N_{10}, but without the growth of the nuclei mode to larger sizes. These increases in N_{10} were often shorter than 1 h and correlated with SO_2, indicating local plumes. An example of a short-lived event is shown in Figure 4.

Alternately, a regional event interrupted by precipitation, significant change in wind direction, or front would be classified as a short-lived event.

Table 1
Instruments used to examine nucleation events in this work

Measurement	Instrument	Notes
Main supersite sampling location, Schenley Park, Pittsburgh (urban site)—Sampled 7/1/01–9/30/02		
Particle size distribution, 3–80 nm	TSI 3085 DMA/TSI 3025A CPC	5 min upscan; 8 scans per hour
Particle size distribution, 13–680 nm	TSI 3081 DMA/TSI 3010 CPC	5 min upscan; 8 scans per hour
Particle size distribution, 0.5–10 μm	TSI 3320 APS	Operated 7/1/01–10/26/01
Particle size distribution, 0.5–10 μm	TSI 3321 APS	Operated 5/26/02–9/30/02
$PM_{2.5}$ mass	R&P 1400A	Running at 30°C with sample equilibration system
Ozone	API 400A	
NO & NO_x	API 200A	
SO_2	API 100A	
CO	API 300A	
Wind speed	MetOne 014A	
Wind direction	MetOne 024A	
Precipitation	MetOne 370	
Temperature and RH	Campbell HMP45C	
Barometric pressure	Campbell CS105	
Downwelling broadband radiation	Kipp & Zonen CM3 Pyranometer	
Downwelling UV radiation	Kipp & Zonen CUV3 UV Pyranometer	
Upwind sampling location, Florence, PA (rural site)		
Particle size dstribution, 12 nm–280 nm	TSI 3071 DMA & 3010 CPC	Sampled 2/24/02–3/28/02

Regional nucleation events were further classified as "weak," "moderate," and "strong," depending on the net rate of increase in N_{10} during the first hour of the event. The divisions were as follows: $dN_{10}/dt < 4{,}000$ cm^{-3} h^{-1} was classified as weak, dN_{10}/dt from 4,000–15,000 cm^{-3} h^{-1} was classified as moderate, and $dN_{10}/dt > 15{,}000$ cm^{-3} h^{-1} was classified as strong nucleation. It should be noted that dN_{10}/dt is not the nucleation rate, typically defined as the number of nuclei clusters growing larger than 1 nm. Rather, this is a rough measure of the intensity of the event and also of its impact on the particle number and size distribution in the region.

One final challenge in distinguishing nucleation from primary particle emission was the observation of growth events, beginning with particles larger than 6 nm, rather than the expected situation of nucleation accompanied by particles down to the instrument detection limit of 3 nm. In these cases, the increase in N_{10} was rather modest and difficult to distinguish from the increase in N_{10} associated with traffic. In all other respects, the events look like the other nucleation events, including an increase in N_{50} (number concentration of particles smaller than 50 nm) significantly above levels seen on days without nucleation and the characteristic growth of the new mode to 30–100 nm in size. An explanation for these events is that nucleation is occurring near the sampling site but not directly at the site, and the particles travel to the site while growing and coagulating. Another possible explanation is that these are primary particles from vehicle emissions that are growing by condensation, and that the increase in N_{50} is explained by an increased lifetime of primary particles due to their larger sizes. Our results support the former explanation for two reasons. First, the sources of primary particles in the 10–20 nm size range are mainly vehicles in and around the city of Pittsburgh. The size of the grown primary particles as sampled would depend on the source distance from the site, the condensational growth rate, and the wind speed. Since the sources are at a constant distance from the site, and the condensational growth rate varies with photochemical activity, one would expect an initial increase in the size of the grown primary particles, and then a decrease later in the day. Such behavior was not observed. The second reason is that the observed increases in N_{50} for stable wind directions are too rapid to be accounted for by increased lifetimes of particles as they grow in size. Therefore, these events have been classified as nucleation events.

Figure 5 shows the overall frequency of days with nucleation activity from July 2001 to June 2002 according to the classification scheme described above. The overall nucleation frequency, counting all event types, was 53%, or 181 of 345 study days. The regional nucleation events occurred during 31% of the study days. Regional nucleation seemed to be more frequent during the spring and fall, and less active in summer and winter. Table 2 summarizes key gas phase, meteorological, and aerosol variables during strong, regional nucleation events.

Spatial Scale of Nucleation

The spatial scale of nucleation was investigated by operating an SMPS in Florence, Pennsylvania (Figure 1) during parts of

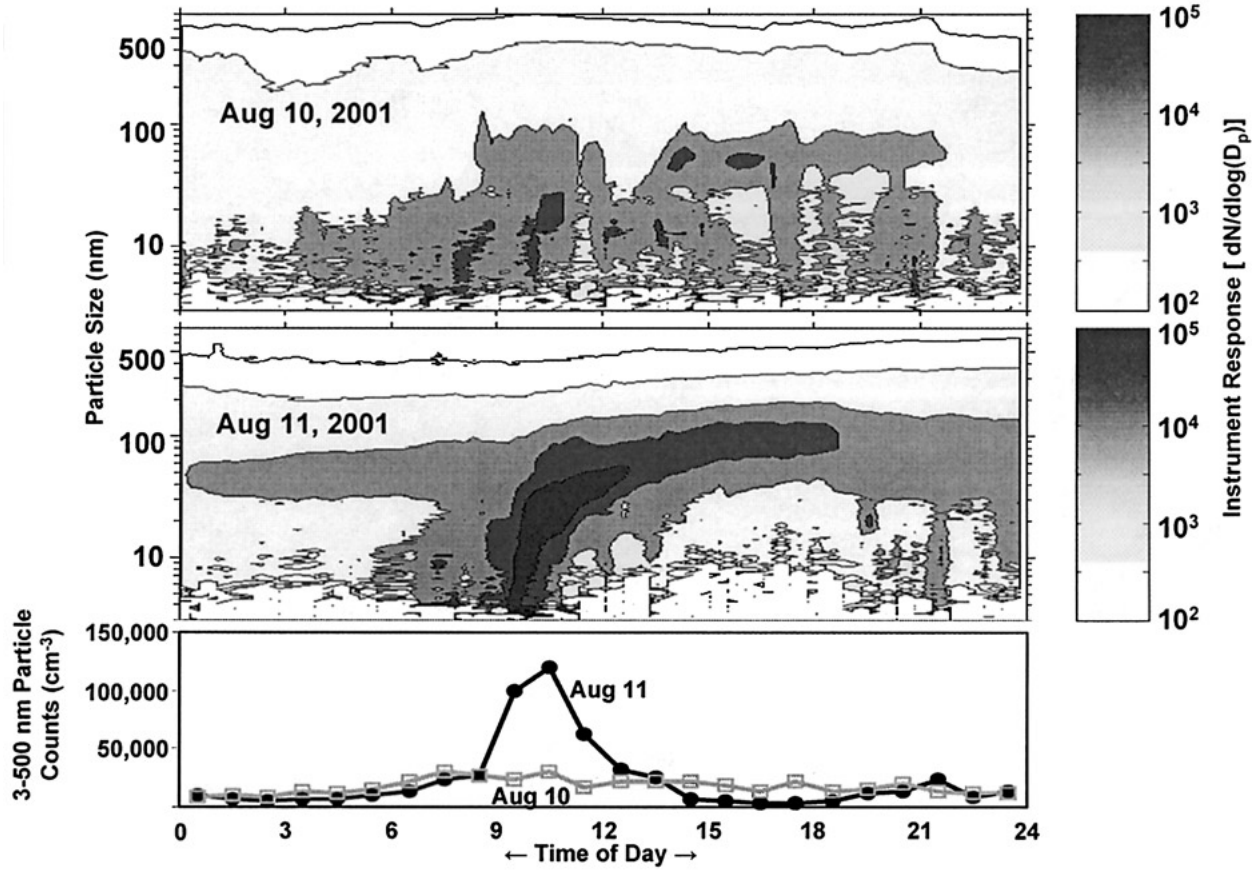

Figure 2. Evolution of particle size distributions and particle concentration on a day without nucleation (10 August) and a day with nucleation (11 August). The top two plots show instrument response over all size channels. The bottom plot shows the integrated particle concentration time series. Nucleation is apparent at 9 am EST on 11 August.

February and March of 2002. This site was 38 km to the west of the main site. Although the lower limit of the size distributions was at 10 nm, the growth portion of the nucleation events was clearly evident and coincided in time well with the events at the main site (Figure 6). On other days of the study, no nucleation occurred at both sites. Of the 34 days of parallel sampling, all of the stronger nucleation events except one happened at both sites at nearly the same time. Only five days show qualitative disagreement between the two sites, usually with weak nucleation at one site but not the other.

Conditions Favorable to Nucleation

Nucleation occurred most frequently on sunny days with below-average $PM_{2.5}$ concentrations (Table 2). This often occurred on days after the passage of a cold front through the area with subsequent high pressure and clear skies. Although this general pattern held, no simple relationship between sunlight, preexisting aerosols, and nucleation was identified. During summer, regional nucleation was mostly associated with light northwesterly winds, while in fall and winter it was mostly associated with stronger southwesterly winds. During spring, the wind direction for nucleation was highly variable.

The hypothesis that these events are due to sulfuric acid nucleation was explored by correlating nucleation activity and H_2SO_4 production. This correlation, based on the ideas of Pirjola et al. (1999) and Wexler et al. (1994), was developed to see how well the observed nucleation events, both short-lived and regional, could be explained in terms of condensation and nucleation of H_2SO_4. As neither OH nor H_2SO_4(g) were measured during PAQS, the product of ultraviolet light and SO_2 was used as a surrogate parameter for H_2SO_4 production. The condensational sink, CS, was calculated from the measured size distribution at near-ambient relative humidity using the formula

$$\mathrm{CS} = \int_{3\,\mathrm{nm}}^{500\,\mathrm{nm}} D_p \beta(D_p) n(D_p) dD_p, \qquad [1]$$

where β is the transitional correction factor (Fuchs and Sutugin 1970), D_p is particle diameter, and $n(D_p)$ is the measured number size distribution. The condensational sink is only integrated through 500 nm because the size distributions extending beyond this size are not available for all time periods of the study. Therefore, this is a low estimate of the actual condensational sink, especially when aged aerosols are sampled.

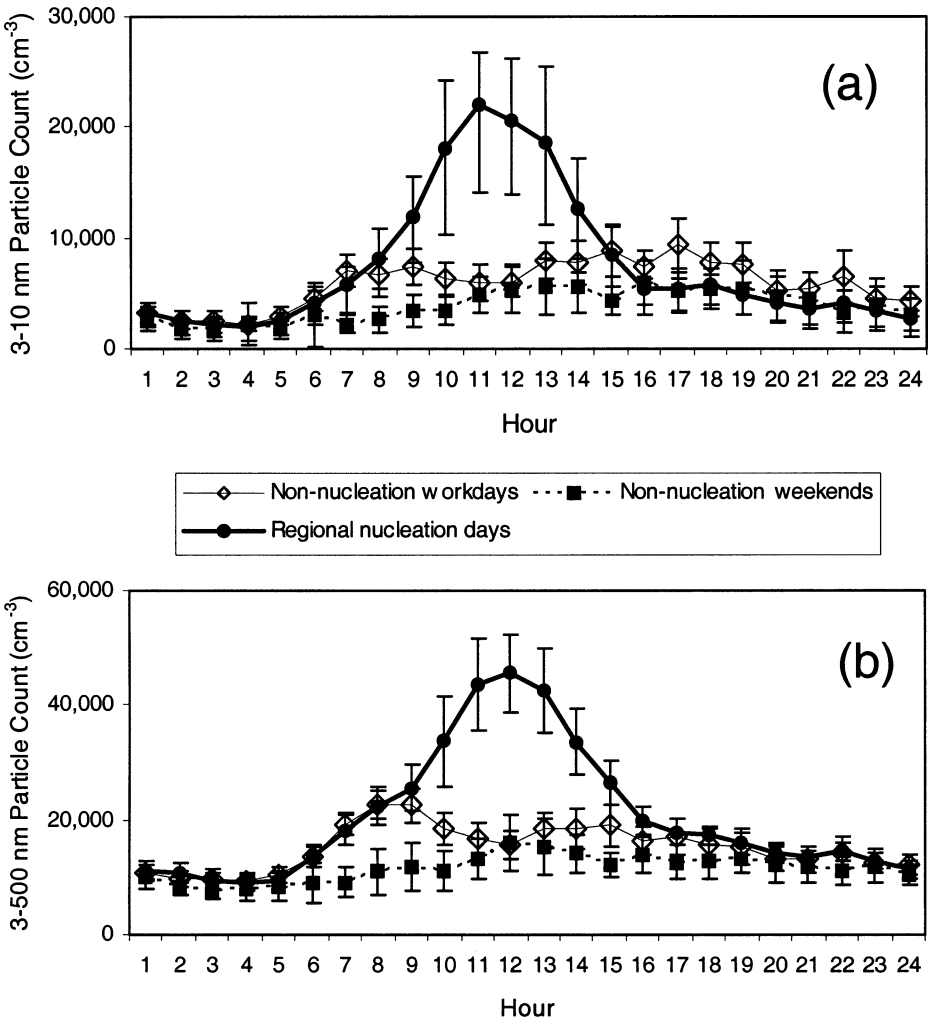

Figure 3. Diurnal averaged number concentrations, July to November 2001. Error bars signify the 95% confidence interval on the mean: (a) particles 3–10 nm, N_{10}, and (b) particles smaller than 500 nm, N_{500}.

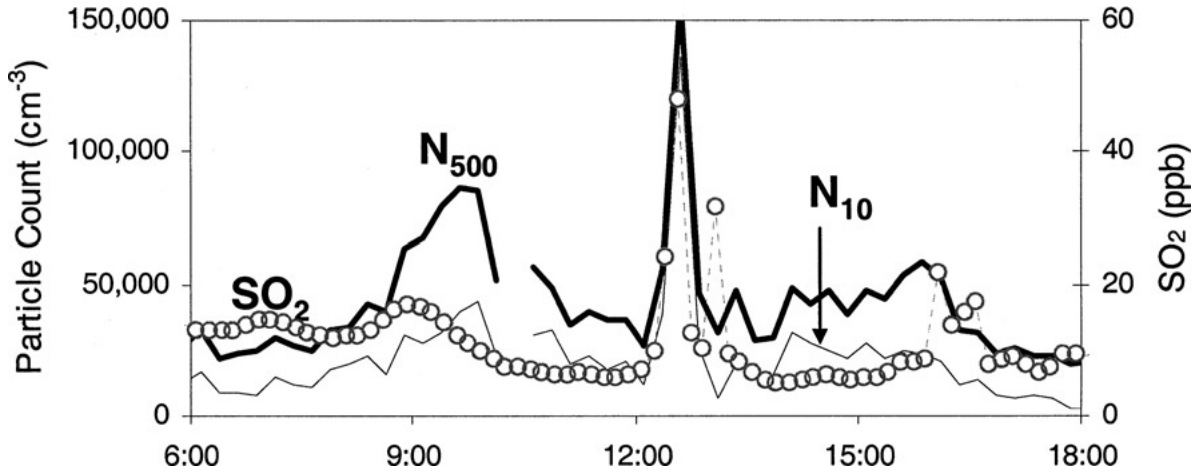

Figure 4. Example of a short-lived nucleation event on 5 July 2001.

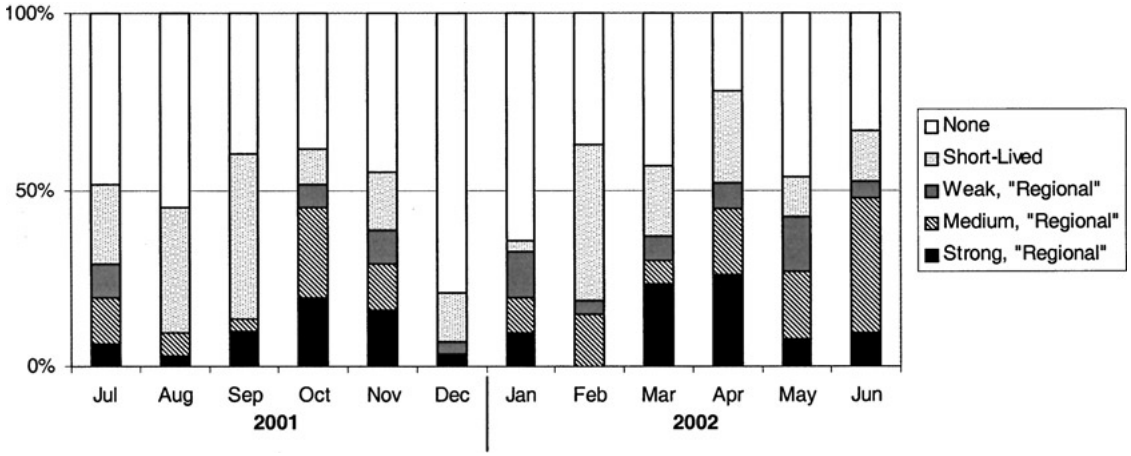

Figure 5. Overall frequency of nucleation. Days are classified by the occurrence of nucleation activity. Weak, medium, and strong refer to the rate of increase of N_{10} during the first hour of the event. $dN_{10}/dt < 4{,}000$ cm^{-3} h^{-1} was classified as weak, dN_{10}/dt from 4,000–15,000 cm^{-3} h^{-1} was classified as moderate, and $dN_{10}/dt > 15{,}000$ cm^{-3} h^{-1} was classified as strong nucleation. Short-lived events refer to nucleation without growth to larger sizes.

The result of the correlation is shown in Figure 7. The panels of Figure 7 can be divided into 2 qualitative regions. The upper left portion of each figure (Region I), dominated by grey points, is where nucleation is relatively rare, because the sulfuric acid production is too slow, or there is too much area available for condensation. The second region is where the bulk of the black points are, indicating conditions more favorable to nucleation. As the UV * SO_2 product increases and the condensational sink decreases, the ratio of nucleation points (in black) to nonnucleation points (in grey) increases. The nucleating conditions do

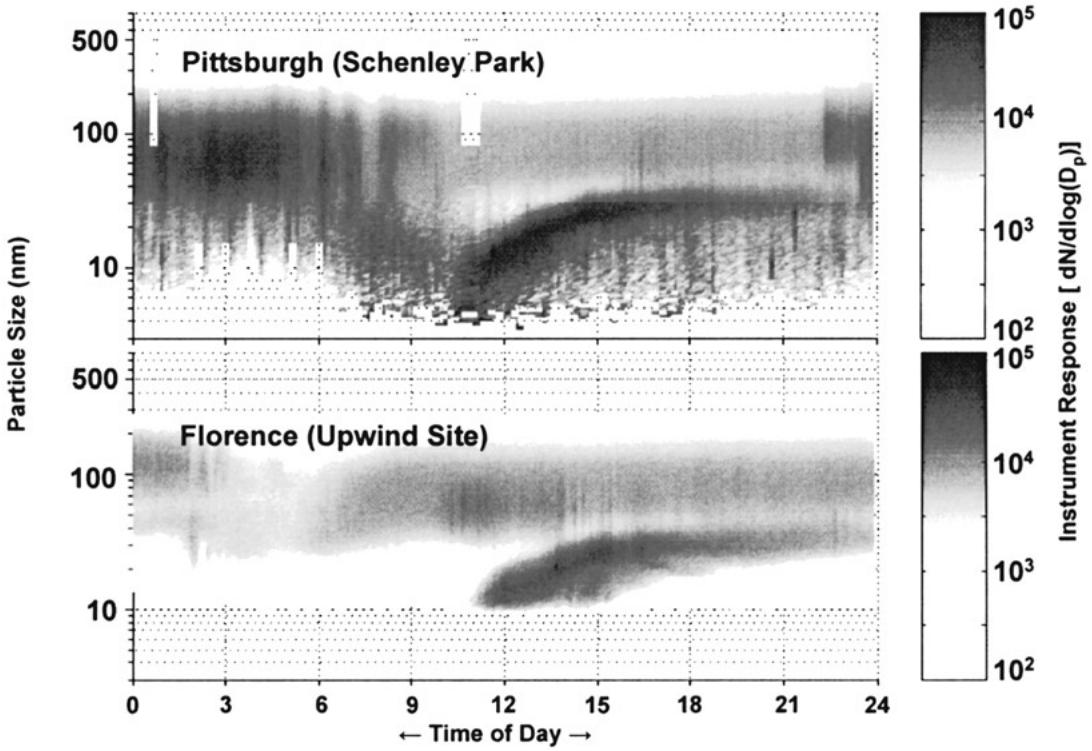

Figure 6. Graphical representation of instrument response for two sites. The top plot shows results at an urban sampling location in Pittsburgh, PA and the bottom graph shows results for the same time period from an upwind, rural site 40 km away. Nucleation is apparent at around 10 am local time.

Table 2
Summary of conditions during strong, regional nucleation events

Date	Time	Strong inversion[a]	RH %	Temp °C	Wind direct. degree	Wind speed m/s	$PM_{2.5}$ TEOM $\mu g/m^3$	Conden. sink cm^{-2}	UV W/m^2	Num. conc. (#/cc)			NO (ppb)			SO_2 (ppb)		
										Before[b]	During[b]	% Change	Before[b]	During[b]	% Change	Before[b]	During[b]	% Change
7/14/01	8:00	Y	72	17.8	318	1.5	10.8	0.021	7.2	2.8E + 04	7.2E + 04	157	10.0	3.6	−64	15.5	4.7	−70
7/27/01	6:00	N	64	14.2	31	0.9	8.5	0.013	1.5	1.3E + 04	4.8E + 04	269	0.6	3.2	446	5.8	7.1	23
8/11/01	9:00	N	67	22.6	331	1.1	8.3	0.021	8.0	na	1.1E + 05	na	2.3	3.9	71	14.3	41.3	188
9/15/01	8:00	N	78	10.1	85	0.0	5.7	0.018	5.9	2.1E + 04	6.9E + 04	229	8.9	10.0	12	0.0	4.4	na
9/16/01	10:15	N	59	17.3	345	1.7	8.6	0.020	22.8	2.0E + 04	8.1E + 04	305	10.4	3.1	−70	0.0	13.8	na
10/8/01	10:30	Y	48	8.3	256	1.5	6.0	0.019	18.4	3.3E + 04	6.0E + 04	82	54.8	8.1	−85	21.8	13.9	−36
10/9/01	10:00	N	45	11.5	135	1.7	22.3	0.042	16.3	3.8E + 04	3.9E + 04	3	75.7	25.7	−66	19.5	46.7	139
10/10/01	9:30	N	44	14.6	162	2.1	13.9	0.023	14.3	2.5E + 04	4.1E + 04	64	22.0	7.1	−68	4.7	7.4	58
10/13/01	9:45	N	73	21.2	129	3.0	9.7	0.020	15.6	2.8E + 04	na	na	20.9	8.9	−57	11.6	22.2	92
10/15/01	8:45	N	72	10.9	263	2.7	9.4	na	9.0	2.4E + 04	5.5E + 04	129	9.4	7.9	−16	9.6	10.0	4
10/18/01	11:45	Y	42	10.7	224	1.9	4.1	0.013	23.4	2.5E + 04	4.8E + 04	92	12.0	5.2	−57	1.2	5.4	347
11/3/01	11:00	Y	54	13.6	289	2.5	9.7	0.022	17.2	3.1E + 04	4.4E + 04	42	19.8	5.9	−70	24.2	9.5	−61
11/4/01	9:00	Y	59	9.5	203	1.8	7.3	0.016	7.2	1.7E + 04	5.5E + 04	224	12.2	4.3	−65	5.7	7.8	38
11/10/01	8:45	N	59	6.5	219	3.0	na	0.020	5.4	1.6E + 04	6.1E + 04	281	5.8	10.5	83	25.8	32.8	27
11/22/01	9:00	N	57	4.9	160	2.1	15.2	0.020	5.1	1.8E + 04	3.9E + 04	117	18.4	10.9	−41	11.7	11.6	−1
12/3/01	11:30	Y	40	12.6	182	2.5	4.0	0.015	13.9	3.0E + 04	6.3E + 04	110	36.8	10.8	−71	11.7	12.9	10
1/25/02	11:30	N	58	2.9	265	3.0	9.0	na	14.6	2.6E + 04	3.9E + 04	50	13.0	10.2	−22	14.2	7.6	−46
1/26/02	9:15	N	56	2.1	183	2.4	9.6	na	5.2	1.6E + 04	4.1E + 04	156	7.4	11.3	54	16.0	15.9	−1
1/27/02	11:00	N	46	10.2	214	2.8	10.1	na	13.7	9.8E + 03	2.9E + 04	196	8.2	8.6	5	12.1	13.7	14
3/7/02	10:30	N	34	10.5	19	0.4	20.1	0.026	10.4	2.4E + 04	4.3E + 04	79	12.0	6.7	−44	18.2	15.1	−17
3/9/02	10:00	N	46	17.7	287	4.2	18.5	0.018	15.1	1.7E + 04	5.9E + 04	247	5.9	4.5	−23	6.6	12.8	94
3/15/02	10:45	N	48	19.4	45	5.2	14.9	0.016	18.0	2.3E + 04	5.7E + 04	148	3.9	3.8	−5	8.1	13.0	60
3/23/02	8:00	N	55	−2.4	35	4.3	6.9	0.013	6.1	1.4E + 04	7.7E + 04	450	2.7	4.3	59	6.6	6.9	5
3/24/02	8:00	N	45	3.4	263	0.1	10.9	0.019	5.0	1.2E + 04	3.1E + 04	158	3.1	4.8	55	12.6	16.1	28
3/29/02	11:00	N	36	17.0	309	2.1	11.8	0.025	26.3	2.2E + 04	5.9E + 04	168	8.2	5.3	−35	9.7	21.6	123
4/2/02	10:45	Y	32	16.3	201	3.6	8.9	0.013	27.1	2.5E + 04	4.3E + 04	72	20.1	5.2	−74	14.6	6.8	−54
4/11/02	10:30	Y	28	17.8	141	4.3	10.2	0.012	27.6	1.9E + 04	5.2E + 04	174	11.4	5.0	−56	5.3	2.6	−52
4/12/02	9:15	N	43	15.0	150	0.5	16.5	0.024	14.7	2.4E + 04	3.9E + 04	63	11.7	8.8	−24	7.1	21.6	203
4/16/02	9:15	Y	54	24.6	220	0.4	26.0	0.026	19.1	3.0E + 04	7.8E + 04	160	23.8	10.0	−58	11.8	17.8	51
4/17/02	9:00	N	52	24.9	249	0.5	31.7	0.029	16.6	na	6.4E + 04	na	84.4	10.1	−88	20.4	17.3	−15
4/18/02	8:45	N	61	22.3	na	0.0	22.8	0.026	12.8	3.1E + 04	5.7E + 04	84	20.0	15.4	−23	11.2	18.7	67
4/27/02	9:15	N	41	11.0	25	0.9	13.4	0.016	18.0	1.4E + 04	4.5E + 04	221	10.5	7.0	−34	4.5	14.1	215
5/11/02	9:30	Y	34	15.0	99	1.8	11.2	0.012	25.3	1.6E + 04	9.2E + 04	475	6.6	4.3	−35	3.5	18.5	427
5/30/02	10:00	Y	57	24.9	288	0.2	26.0	0.027	24.6	4.4E + 04	5.2E + 04	18	6.9	5.5	−20	8.5	17.8	109
6/3/02	8:45	Y	48	16.6	na	0.0	13.5	0.021	8.1	7.6E + 04	1.3E + 05	71	12.0	8.9	−26	7.8	19.8	153
6/22/02	9:00	Y	52	25.2	187	1.5	31.0	na	16.4	na	na	na	10.2	4.7	−54	10.8	16.0	49
6/24/02	9:00	Y	55	27.0	199	1.2	32.3	na	15.1	na	na	na	22.6	11.5	−49	25.5	54.1	112

[a] Y refers to days when a clear breaking of the nighttime inversion could be identified at approximately the same time as the inception of nucleation. Breaking of the inversion was identified as a sharp drop in ground-level $PM_{2.5}$, NO, RH, and CO (Figure 9). N refers to days when the inversion layer was either not present or not significant enough to detect by analyzing the time series.

[b] Before is calculated as the average of the 2 h period prior to nucleation. After is calculated as the average of the 2 h period beginning with the nucleation event.

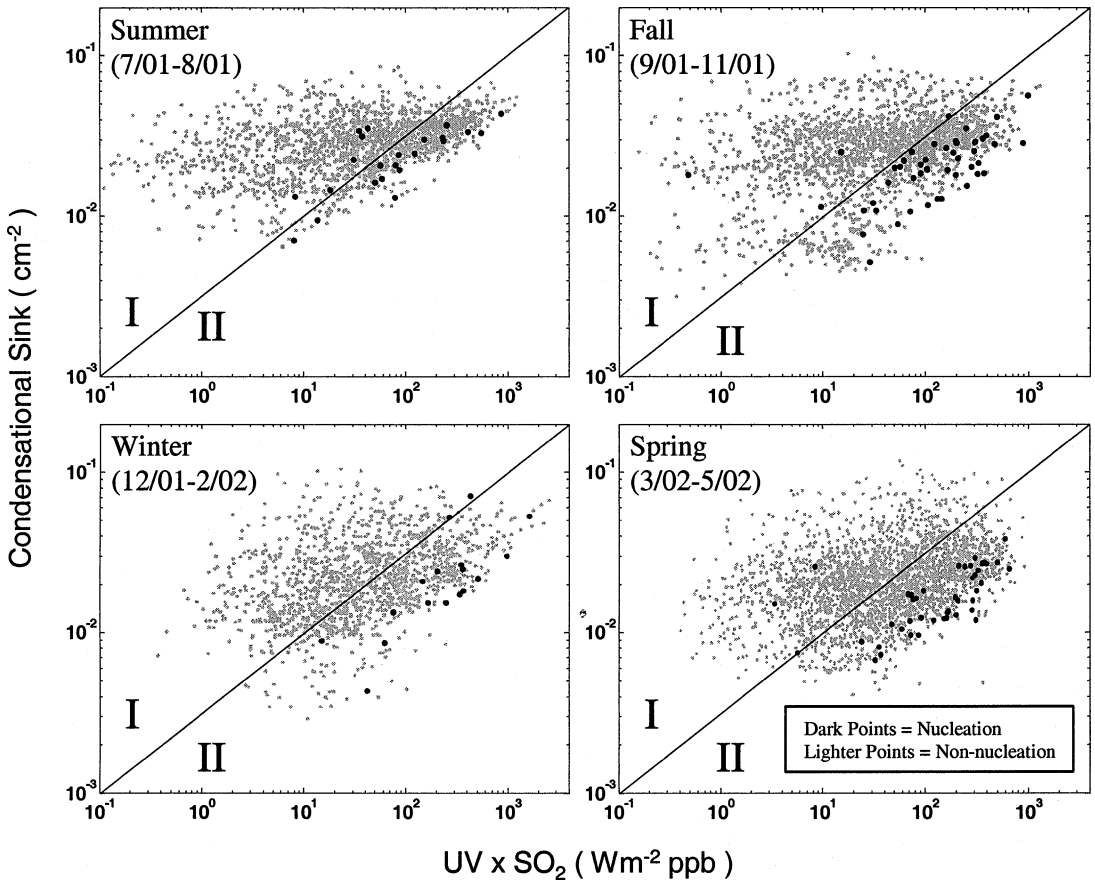

Figure 7. Correlation showing UV * SO_2 versus condensational sink for four different seasons. Condensational sink (y axis) is plotted against the product of ultraviolet light intensity and SO_2 concentration (x axis), a proxy for sulfuric acid production. Fifteen-minute averaged values are plotted for all time periods of the study. The black symbols correspond to onset of nucleation. The grey symbols correspond to periods when nucleation is not observed. The 45 degree line roughly divides each plot into two regions—the upper left region I where nucleation is not generally observed, and the lower right region II where nucleation is more common.

not form a sharp line in this plot. While this is partly due to measurement errors and difficulty in assigning a precise start time to nucleation, it is probably mostly due to additional predictive variables that are important to nucleation. During summer, nucleation takes place at higher condensational sink values for the same value of UV * SO_2. Known variables that should be important include temperature and relative humidity.

The nucleation measurements made during this study are compared to model-based correlations of Pirjola et al. (1999) and Wexler et al. (1994) in Figure 8. Condensational sink (y axis) is plotted against the product of ultraviolet light intensity and SO_2 concentration (x axis), a proxy for sulfuric acid production. These models were designed to predict the required H_2SO_4 production rates for nucleation and growth by H_2SO_4 as a function of condensational sink, relative humidity, and temperature. The observed nucleation events are plotted as solid black circles, while the black lines are the correlation-based thresholds for H_2SO_4 nucleation, with nucleation expected to the right of the lines and not expected to the left. These thresholds are calculated at representative ground-level RH and temperature values. The lines are calculated using some assumptions, including (1) a proportional relationship between UV and OH, with full summer sun of 36 Wm^{-2} UV corresponding to an OH concentration of 10^7 molec cm^{-3}; and (2) a SO_2 deposition characteristic time of 10^4 s (Wexler et al. 1994). With our assumed OH levels, both of the correlations suggest that the ground-level conditions are several orders of magnitude more polluted than those required to induce binary nucleation and growth of fresh particles by sulfuric acid.

Also plotted are grey points, which are model predictions for the critical condensational sink level at OH, SO_2, temperature, and RH levels matching those of the specific nucleation events. This provides a better comparison of models to observations, because a representative RH and temperature is not needed. Each observation (black circle) is matched by 4 grey points, at the same point on the x axis but with different condensational sink values. Grey points refer to the correlations of Wexler et al. (1994) (triangles) and Pirjola et al. (1999) (squares).

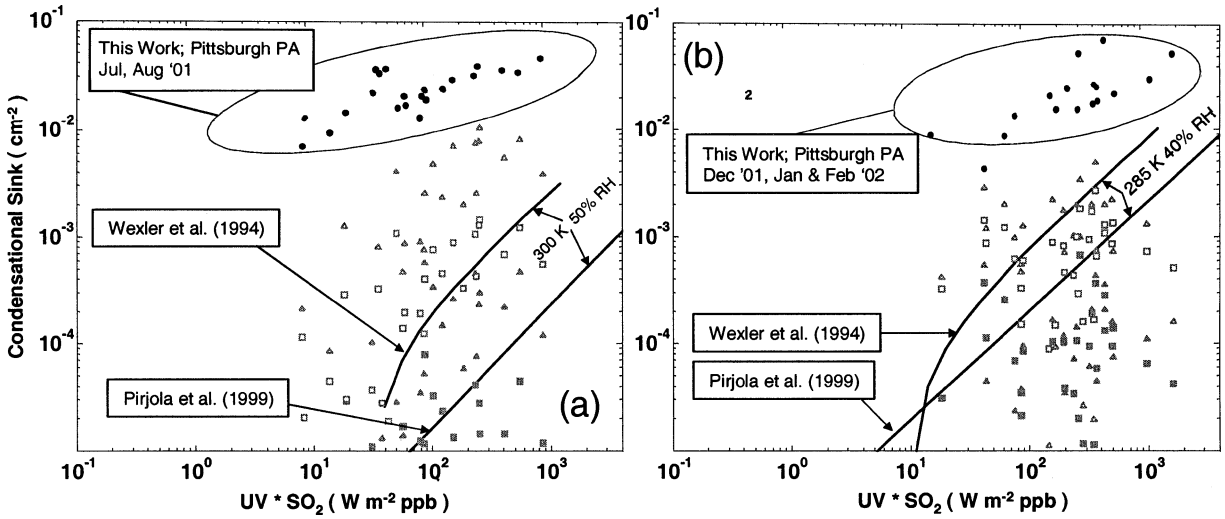

Figure 8. Comparisons of conditions during (a) summer and (b) winter nucleation to model-based correlations for sulfuric acid particle formation from Pirjola et al. (1999) and Wexler et al. (1994). Condensational sink (y axis) is plotted against the product of ultraviolet light intensity and SO_2 concentration (x axis), a proxy for sulfuric acid production. Measured nucleation events (dark circles) are found at the highest condensational sink values. Solid lines refer to correlation predictions for the nucleation threshold at a representative ground-level RH and temperature (nucleation favored to the right of the lines, and not expected to the left). Additional correlation predictions (grey data points) are plotted to see if data-model agreement improves when specific RH and temperature values for each nucleation event are used in the models (triangles = Wexler et al. (1994); squares = Pirjola et al. (1999)). Filled symbols refer to RH and temperature at ground level; unfilled symbols refer to estimated conditions at the top of the boundary layer.

Filled grey symbols are calculated at ground-level meteorological conditions, while open grey symbols are calculated at reduced temperatures and elevated RHs corresponding to the top of the mixed layer. This is done to check if conditions at the top of the mixed layer would be sufficient for sulfuric-acid–induced nucleation. Key assumptions included constant vertical profiles of dewpoint, OH, and SO_2 in the mixed layer, summertime afternoon mixing heights of 2000 m, wintertime afternoon mixing heights of 800 m, and adiabatic cooling of air parcels at a rate of 9.8°C km^{-1}. Using these assumptions, the gap between

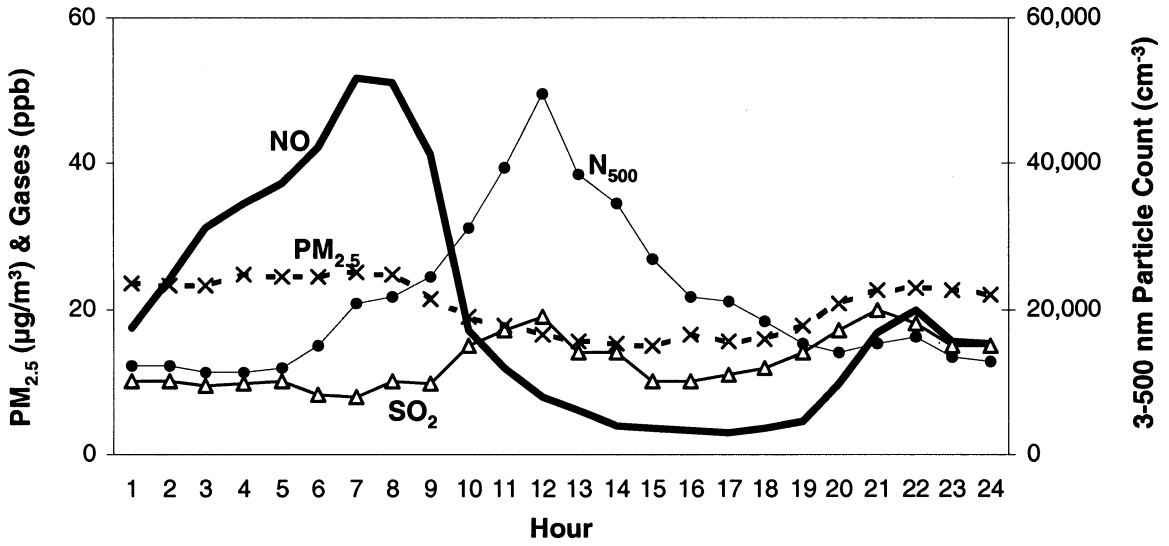

Figure 9. Diurnal profile for inversion-related nucleation. Inversion-related nucleation events from July to November 2001 are averaged. Boundary layer mixing height increases during the mornings, with decreases in $PM_{2.5}$ and NO, increases in SO_2 levels, and nucleation activity.

model predicted and observed condensational sink levels during nucleation narrowed but did not close.

The conclusions that can be drawn from comparing the nucleation models with the PAQS observations (Figure 8) are as follows: (1) observed nucleation is occurring at significantly higher levels of pre-existing aerosol surface area and/or lower levels of sulfuric acid production than predicted by the models; (2) this gap between models and observations is narrowed, but not removed, when lower temperatures and higher RHs at the top of the mixing layer are taken into account; and (3) the observations are not nearly as dependent on meteorology and sulfuric acid production rate as the models are. These conclusions suggest that additional factors, currently absent from the models, such as ammonia chemistry or growth by organic compounds, are involved in the nucleation events.

Many nucleation events were seen to coincide in time with the breakup of the morning inversion. In Table 2, nucleation events where this was especially prominent are noted in the inversion column. Nucleation concurrent with inversion layer breakup is most common in spring and fall. It is not common in winter, possibly due to higher average wind speeds during nucleation events. Figure 9 shows the average diurnal profile for regional nucleation events associated with inversion breakup. The key features of Figure 9 are the unusually high morning peak of NO, significant decrease in $PM_{2.5}$ during the morning, and an increase in SO_2 and NO decreases. This indicates the possibility of nucleation occurring aloft in a SO_2-enriched and low $PM_{2.5}$ stable layer, followed by the mixing downward of the nuclei.

SUMMARY AND CONCLUSION

Continuous particle-size distribution measurements for one year during the PAQS indicate a high frequency of nucleation activity in the region, with nucleation occurring on about 50% of days and regional nucleation events occurring on 30% of days on average. Nucleation occurred during all seasons but was most intense during spring and fall. The nucleation events are more probable during bright sunny conditions with elevated SO_2 concentrations and low pre-existing aerosol surface area. This relationship was analyzed using a simple correlation of UV * SO_2 versus condensational sink and compared to existing correlations for binary H_2SO_4-H_2O nucleation. The correlation indicated that nucleation occurs under higher aerosol loading conditions and/or with lower H_2SO_4 production rates than expected. A few events that did not follow the overall pattern appear to be influenced by conditions that made classification of the events problematic, such as a weak nucleation rate or a frontal passage. The correlation between H_2SO_4 production and nucleation activity provides strong evidence that sulfate plays a major role in new particle formation in Western Pennsylvania. The difference between the model-predicted and observed nucleation frequencies indicates that additional compounds, such as ammonia or organics, are possibly involved in the nuclei formation and/or growth in addition to sulfuric acid.

REFERENCES

Allen, A. G., Grenfell, J. L., Harrision, R. M., James, J., and Evans, M. J. (1999). Nanoparticle Formation in Marine Airmasses: Contrasting Behaviour of the Open Ocean and Coastal Environments, *Atmos. Res.* 51:1–14.

Birmili, W., Wiedensohler, A., Heintzenber, J., and Lehmann, K. (2001). Atmospheric Particle Number Size Distribution in Central Europe: Statistical Relations to Air Masses and Meteorology, *J. Geophys. Res.* 106(D23):32,005–32,018.

Charlson, R. J., Lovelock, J. E., Andreae, M. O., and Warren, S. G. (1987). Ocean Phytoplankton, Atmospheric Sulfur, Cloud Albedo and Climate, *Nature* 326:655–661.

Eisele, F. L., and McMurry, P. H. (1997). Recent Progress in Understanding Particle Nucleation and Growth, *Philos. Trans. R. Soc. London, Ser. B.* 352(1350):191–200.

Fuchs, N. A., and Sutugin, A. G. (1970). *Highly Dispersed Aerosols*. Ann Arbor Science, Ann Arbor, MI.

Harrison, R. M., Grenfell, J. L., Allen, A. G., Clemitshaw, K. C., Penkett, S. A., and Davison, B. (2000). Observations of New Particle Production in the Atmosphere of a Moderately Polluted Site in Eastern England, *J. Geophys. Res.* 105:17,819–17,832.

Harrison, R. M., Jones, M., and Collins, G. (1999a). Measurements of the Physical Properties of Particles in the Urban Atmosphere, *Atmos. Environ.* 33:309–321.

Harrison, R. M., Shi, J. P., and Jones, M. R. (1999b). Continuous Measurement of Aerosol Physical Properties in the Urban Atmosphere, *Atmos. Environ.* 33:1037–1047.

Jang, M. S., and Kamens, R. M. (2001). Atmospheric Secondary Aerosol Formation by Heterogeneous Reactions of Aldehydes in the Presence of a Sulfuric Acid Aerosol Catalyst, *Environ. Sci. Technol.* 35(24):4758–4766.

Kerminen, V. M. (1999). Roles of SO_2 and Secondary Organics in the Growth of Nanometer Particles in the Lower Atmosphere, *J. Aerosol Sci.* 30(8):1069–1078.

Kim, C. S., Adachi, M., Okuyama, K., and Seinfeld, J. H. (2002). Effect of NO_2 on Particle Formation in SO2/H2O/air Mixtures by Ion-Induced and Homogenous Nucleation, *Aerosol Sci. Technol.* 36(9):941–952.

Kulmala, M., Pirjola, L., and Makela, J. M. (2000). Stable Sulphate Clusters as a Source of New Atmospheric Particles, *Nature* 404(6773):66–69.

Kulmala, M., Hameri, K., Aalto, P. P., Makela, J. M., Pirjola, L., Nilsson, E. D., Buzorius, G., Rannik, U., Dal Maso, M., Seidl, W., Hoffman, T., Janson, R., Hansson, H. C., Viisanen, Y., Laaksonen, A., and O'Dowd, C. D. (2001). Overview of the International Project on Biogenic Aerosol Formation in the Boreal Forest (BIOFOR), *Tellus. Ser. B.* 53:324–343.

Novakov, T., and Penner, J. E. (1993). Large Contribution of Organic Aerosols to Cloud Condensation Nuclei Concentrations, *Nature* 365:823–826.

Oberdorster, G., Gelein, R. M., Ferin, J., and Weiss, B. (1995). Association of Particulate Air Pollution and Acute Mortality: Involvement of Ultrafine Particles, *Inhal. Toxicol.* 7:111–124.

O'Dowd, C. D., Aalto, P., Hmeri, K., Kulmala, M., and Hoffmann, T. (2002). Aerosol Formation: Atmospheric Particles from Organic Vapours, *Nature* 416:497–498.

O'Dowd, C. D., Lowe, J. A., and Smith, M. H. (1999). Coupling Sea-Salt and Sulphate Interactions and its Impact on Cloud Droplet Concentration Predictions, *Geophys. Res. Lett.* 26(9):1311–1314.

Peters, A., Wichmann, E., Tuch, T., Heinrich, J., and Heyder, J. (1997). Respiratory Effects are Associated with the Number of Ultrafine Particles, *Am. J. Respir. Crit. Care Med.* 155:1276–1383.

Pirjola, L., Kulmala, M., Wilck, M., Bischoff, A., Stratmann, F., and Otto, E. (1999). Formation of Sulphuric Acid Aerosols and Cloud Condensation Nuclei: An Expression for Significant Nucleation and Model Comparison, *J. Aerosol Sci.* 30(8):1079–1094.

Rivera-Carpio, C. A., Corrigan, C. E., Novakov, T., Penner, J. E., Rogers, C. F., and Chow, J. C. (1996). Derivation of Contributions Sulfate and Carbonaceous Aerosols to Cloud Condensation Nuclei from Mass Size Distributions, *J. Geophys. Res.* 101:19,483–19,493.

Schwartz, J., Dockery, D. W., and Neas, L. M. (1996). Is Daily Mortality Associated Specifically with Fine Particles? *J. Air Waste Manag. Assoc.* 46:927–939.

Shi, J. P., Evans, D. E., Khan, A. A., and Harrison, R. M. (2001). Source and Concentration of Nanoparticles (<10 nm diameter) in the Urban Atmosphere, *Atmos. Environ.* 35:1193–1202.

Shi, Q. (2003). Aerosol Size Distributions (3 nm to 3 μm) Measured at the St. Louis Supersite (4/1/01–4/30/02), M.S. Thesis, Department of Mechanical Engineering, University of Minnesota, Minneapolis, MN.

Stanier, C., Khlystov, A., Chan, W. R., Mandiro, M., and Pandis, S. N. (2004). A Method for the In-Situ Measurement of Fine Aerosol Water Content of Ambient Aerosols: The Dry-Ambient Aerosol Size Spectrometer (DAASS), *Aerosol Sci. Technol.* 38:215–228.

Weber, R. J., McMurry, P. H., Mauldin, L., Tanner, D., Eisele, F., Clarke, A. D., and Kapustin, V. N. (1999). New Particle Formation in the Remote Troposphere: A Comparison of Observations at Various Sites, *Geophys. Res. Lett. Atmos. Sci.* 26:307–310.

Wexler, A. S., Lurmann, F. W., and Seinfeld, J. H. (1994). Modelling Urban and Regional Aerosols—I. Model Development, *Atmos. Environ.* 28(3):531–546.

Woo, K. S., Chen, D. R., Pui, D. Y. H., and McMurry, P. H. (2001). Measurement of Atlanta Aerosol Size Distributions: Observations of Ultrafine Particle Events, *Aerosol Sci. Technol.* 34:75–87.

Zhang, K. M., and Wexler, A. S. (2002). A Hypothesis for Growth of Fresh Atmospheric Nuclei, *J. Geophys. Res.* 107:4577, DOI: 10.1029/2002JD002180.